A NEW PLANAR SAS APPROACH, P-SAS, FOR 3D IMAGING SONAR

A. Belkacem[+], K. Bebes[+], and M.E. Zakharia[#]
+ Faculté des Sciences de Monastir (LIP) Av. de l'environnement, Monastir, 5019, TUNISIA
#Institut de Recherche de l'École Navale, Groupe Acoustique Sous-Marine, EA 3634,
BP600, Brest Armées, 29240, FRANCE
afif_bel@yahoo.fr

Abstract
Synthetic aperture sonar, SAS, has been mainly applied to sidescan sonar geometry with a 1D scanning of the bottom and a synthesis on a linear track. The extension of the method to a 2D scanning leading to 3D images is investigated in this paper. This planar SAS approach, P-SAS will be illustrated for vertical sounder (or sub-bottom profiler) geometry. It can nevertheless be extended to any geometry such as sidescan sonar or multibeam sounder. It can also be viewed as an improvement of image "mosaic" building by introducing a phase in the procedure and lead to coherent mosaic. An algorithm is presented for reducing the computation load that is based on geometry separation. The imaging method has been validated on both simulation and scaled tank data. The relevance of the planar approach is shown for both proud and buried target's case.

Introduction

SAS processing is becoming more and more popular since several autofocusing algorithms have been developed. Its use has mainly been restricted to sidescan sonar, in particular for mine hunting. The SAS approach can, nevertheless, be applied to any other geometry, in particular planar one, P-SAS.

Planar SAS, P-SAS

Let us consider a down-looking transducer scanning a plane surface with sampling intervals Δx and Δy. For a point target, the echoes will be situated on a hyperbolic surface (figure 1). The range to the target will vary with both X and Y coordinates with a minimum R_0 when the transducer is just above the target.

Planar SAS, P-SAS, is a 2D extension of linear SAS, L-SAS (1D), where the same general principles will be applied [2]. It will consist, for every time sample and for every position, in searching for all the corresponding samples on the migration hyperbolic surface and adding them coherently. Dynamic focusing, commonly used in 1D SAS [1], can also be applied: in both X and Y directions, the number of platform positions used for focusing will be proportional to the target range. The angular resolution will thus be constant with range and equal to about half the physical array in all directions. The principle of P-SAS focusing is illustrated in figure 2. Let Nx be the number of platform positions used in X and Ny the one in Y. Both will be proportional to target range. We can easily see that, for every time and position, the computational complexity (number of search and additions) is proportional to Nx . Ny.

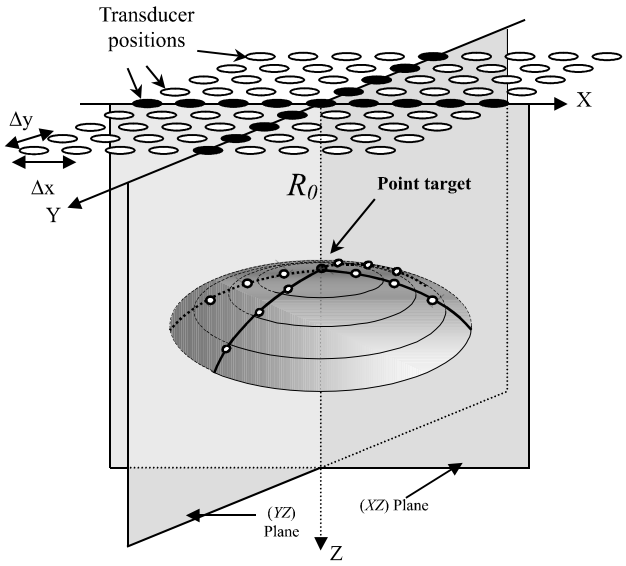

Figure 1: Planar SAS geometry

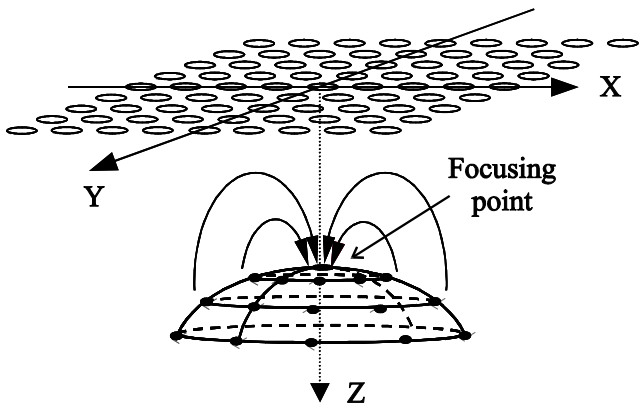

Figure 2: Principle of planar SAS processing

Reduction of processing complexity

As we have seen in the previous paragraph, the complexity of the processing increases with the square of the target range R_0. In conventional SAS, this will be proportional to the range. In order to reduce the processing complexity, we have developed a specific algorithm inspired from the 2D FFT one [4]. This algorithm is illustrated in figure 3.

The raw data are provided in the form of a "cubic" matrix with X, Y and Z indexes. The size of this matrix is defined by the maximum range considered. Its vertical "height" is defined by the range of variation of the target position.

Instead of applying the focusing algorithm to the raw data matrix E, the proposed algorithm will carry out the focusing in two steps:

- A linear SAS will be applied along the X direction leading to the S_x matrix
- A linear SAS will then be applied along the Y direction to the data of the S_x matrix leading to a S_{xy} matrix focused in both directions.

The proposed planar SAS algorithm is presented in figure 3. It will be called 2.2D focusing (in contrast with 3D).

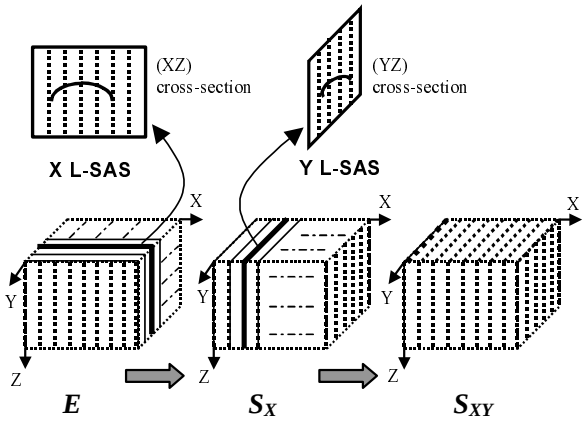

Figure 3:Planar SAS processing algorithm

If we consider a Nx by Ny matrix, the computation complexity will be Nx + Ny instead of Nx . Ny For a square matrix Nx= Ny = N, the complexity reduction will be N/2. The computation load becomes proportional to the target range (and not its square) as in the case of linear SAS. It is worthwhile mentioning that the reduction rate does not depend on the algorithm used for focusing.

Simulations

Simulations have been carried out in order to validate the algorithm and evaluate the performance loss before applying it to experimental data sets. Figure 4 shows an example of raw data represented in 3D. One can clearly see the migration of the echo on a hyperbolic surface. The cross-section of this surface is a hyperbola migration path commonly encountered in linear SAS.

Both fully 3D focusing and 2.2D algorithm have been applied to raw data.

Figures 5 shows the comparison of the focusing performance between these two processing. As one can see, the difference is small. Cross-section have been computed, at the target position, in order to study the difference in details (figure 6). From figure 6 one can see that the resolution is quite the same. There is a loss in the peak value of about 1.5 dB and a slight increase in side lobe level (although they remain lower than 30 dB, which still remains acceptable).

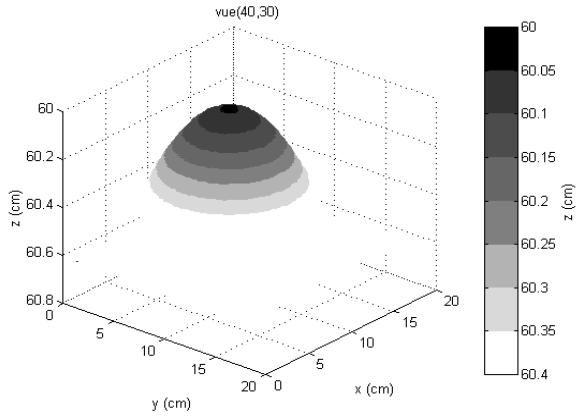

Figure 4: example of raw data

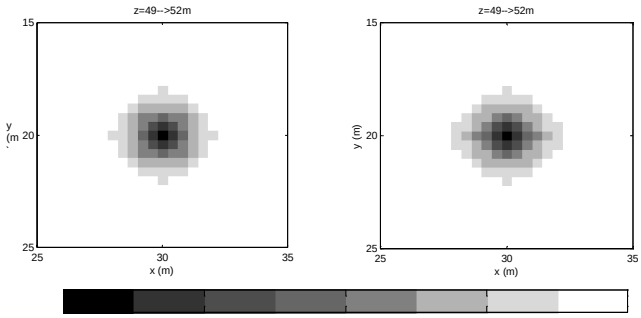

Figures 5: 3D (left) vs. 2.2D (right) processing

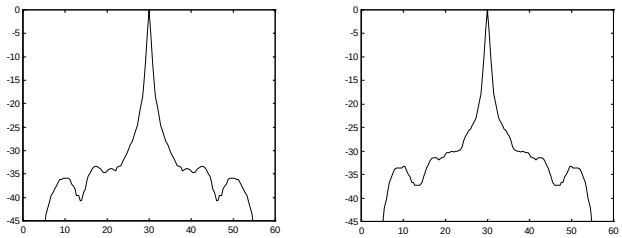

Figure 6: cross-sections of the images presented in figure 5 at target position; 3D (left) 2.2D (right)

Tank experiment

A tank experiment has been conducted in a tank with a computer controlled displacement system.

The dimensions of the water tank are about: 2 m. length, 1 m. large and 1 m. depth. The first experiment used four identical glass spheres of 1.6 cm in diameter lying on a plane sandy bottom.

The transmitted signal is a tone burst centred at 1.1

MHz (two periods). The transducer bandwidth ranges from 800 to 1450 kHz. It possesses a diameter of *D=0.6 cm* and is placed at about 60 cm from the bottom. A 2D scanning was achieved covering an area of 20 cm x 18 cm, with a 0.2 cm step for both directions (X and Y).

While scanning the whole area, 9191 signals were obtained, corresponding to all the transducer's positions.

These signals constitute a 3D matrix possessing the following size:

- Nx =101 positions,
- Ny =91 positions and
- Nz = 8192 samples.

The experiment geometry is shown in figure 7. The same scanning geometry was used, later on, for buried targets.

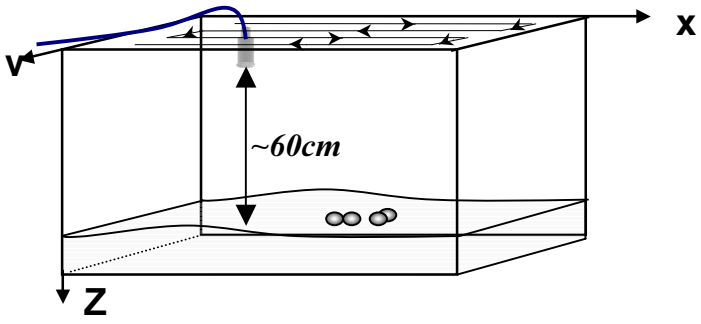

Figure 7: Tank experiment geometry

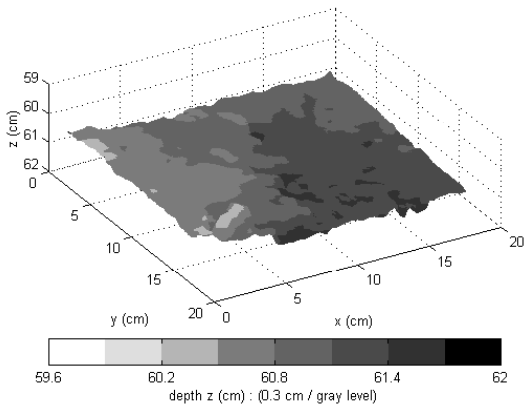

Figure 8: Planar SAS, raw data, tank experiment

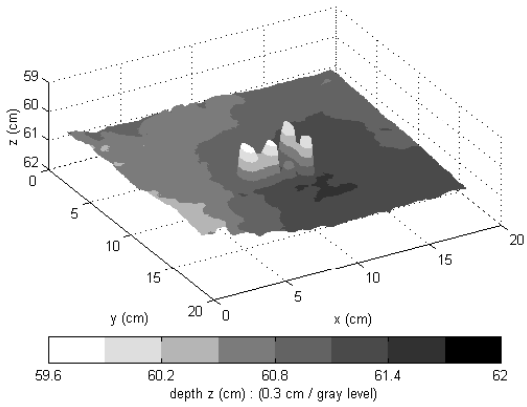

Figure 9: Planar SAS, processed data, tank experiment

Figure 8 shows the raw data obtained in a conventional 3D plot (the depth corresponding to the first echo is plotted for every ping). The same plot is used for processed data, in figure 9. The resolution improvement is clear in both X and Y directions.

When comparing 3D P-SAS to 2.2. P-SAS on this experimental example, the resolution is quite comparable for both processing techniques, while the gain in computation time is about 30. As shown in figure 10, the resolution obtained by both algorithms is quite comparable.

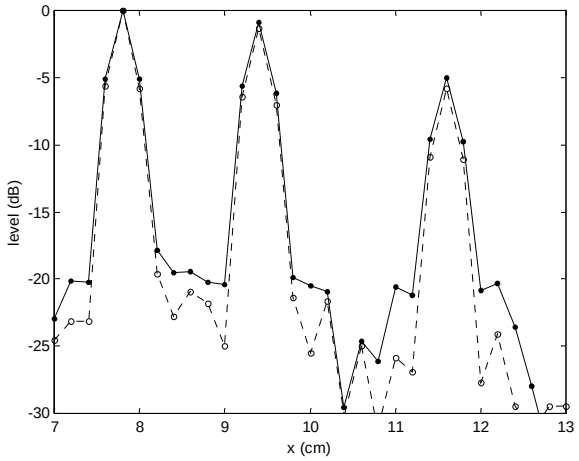

Figure 10: Cross-section of image of figure 9 computed at target position.
Solid line: 3D P-SAS, Dashed line: 2.2D P-SAS.

After the validation of planar SAS on both simulations and proud targets imaging (or interface mapping), we have investigated its possible application to buried targets. Several simulation have shown that, for judicious geometry set ups, the defocusing in the sediment can be neglected and that focusing can be achieved as if the sediment possessed the same properties as water [3].

Another tank experiment has been conducted using the experimental geometry of figure 7. A hollow air-filled cylinder (diameter = 2.5 cm, length = 2.6 cm) was buried in a sand layer at about 10 mm from the interface.

Representing sub-bottom data cannot be achieved using conventional 3D plots as they will pick up the first echo (interface) and ignore the buried target echo. A less conventional display system has been used which consists in "strata" display. It consists in a series of images corresponding to the integrated received energy in a given strata (time window). Images are displayed in sequence; vertical scale corresponds to Y direction, horizontal scale to X direction and the image number (or position) the Z axis (stratum boundaries). The received energy is coded in grey levels (or colours). The results obtained on a buried cylinder are shown in figures 11 representing a vertical down-looking view.

The strata depth interval is given on the top of each image. The last image shows a drawing of cylinder position and size. The cylinder is situated in oblique incidence on purpose in order to avoid any geometrical or sampling artefact (its generating line is not parallel to any scanning axis).

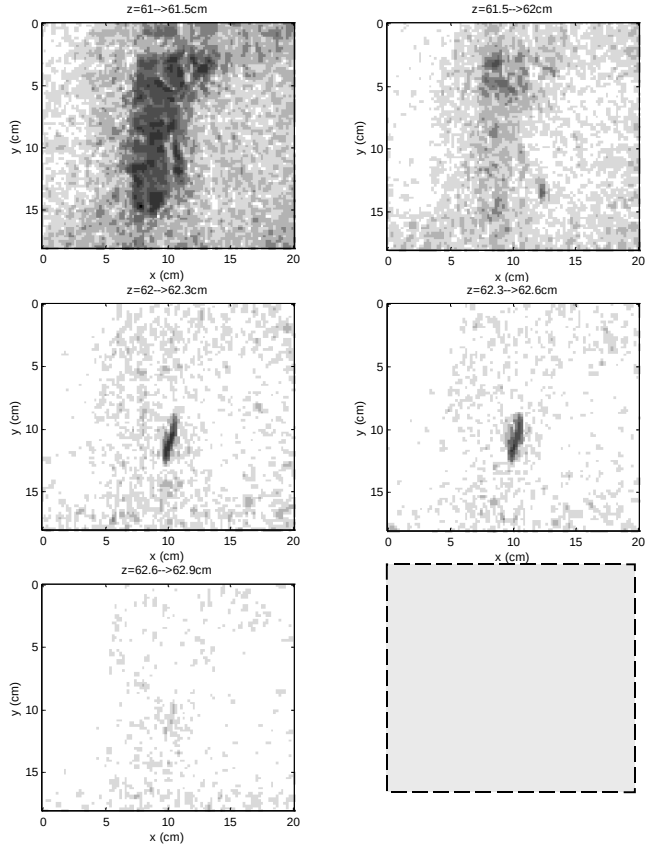

Figure11: Strata display of P-SAS imaging of a buried target (from left to right and from top to bottom)

From these images, the cylinder echoes can be easily separated from the interface one and, from all these echoes, the major characteristics of the target can be estimated. These results are summarised in table 1.

Table 1 : Target parameters

Parameter	Actual value	Estimated value
X position	100 mm	100 mm ± 2 mm
Y-position	110 mm	110 mm ± 2 mm
Z-position	~610 mm	623 mm ± 0.05 mm
Burial depth	10 mm	8.9 mm ± 0.1 mm
Length	26 mm	27 mm ± 2 mm
Width	25 mm	4 mm ± 2 mm

The target length and width were measured for a –6 dB attenuation. As we can see in table 1, most of the geometrical characteristics of the buried target could be estimated with a good accuracy except the diameter. In fact, what we called the target width is the duration of the echo corresponding to the specular echo on its generating top line. As no penetration in the object was possible, the echo corresponding to the bottom generating line was absent..

Conclusion

The results obtained for both simulation and tank experiment data have shown the relevance, in a sounder geometry, of P-SAS techniques for imaging both proud and buried targets. The method proposed for reducing the computation complexity has been validated on both simulations and tank data. From the "strata" display, the main characteristics of the targets could be extracted.

Several issues still have to be investigated. The first one is the extension to other geometrical set ups and the application of the method to "coherent mosaic" set up. The second one is the influence of the platform instabilities on the final image quality and the means to correct it. Although the trajectory geometry is a 3D one, we will try to split it in 2D components and correct in sequence the X L-SAS and the Y L-SAS.

References

[1] M. E. Zakharia, and J. Chatillon, "synthetic aperture mapping and imaging". *Chap. 2 of Underwater Acoustic Digital Signal Processing and Communication Systems*. Edited by R. S. H. Istepanian and M. Stojanovic. Kluwer Academic Publishers. pp. 37-88.

[2] Afif Belkacem, Kamel Besbes, Jacques Châtillon, and Manell E. Zakharia. "Planar Synthetic Aperture for sea Bottom and Sub-bottom Imaging", submitted to IEEE Ocean Engineering Journal

[3] Afif Belkacem, Kamel Besbes, Manell E. Zakharia "Defocusing Error in SAS Sub-bottom Imaging", tenth international Congress on Sound and Vibration, 7-10 July 2003, Stockholm, Sweden.

[4] L. Rabiner and B. Gold, "Theory and application of digital signal processing", Prentice Hall, 1975.

Acknowledgements

This work was partly supported by the European Commission, EC funded SITAR project (Seafloor Imaging and Toxicity; Assessment of Risks caused by buried waste) project number EVK3-CT-2001-00047.